Copy 45
RM SL52F20

NACA

RESEARCH MEMORANDUM

for the

Air Materiel Command, U. S. Air Force

AN INVESTIGATION OF THE EFFECT OF THE WADC 30,000-HORSEPOWER WHIRL RIG UPON THE STATIC CHARACTERISTICS OF A PROPELLER

By Leland B. Salters, Jr., and Harry T. Norton, Jr.

Langley Aeronautical Laboratory
Langley Field, Va.

NATIONAL ADVISORY COMMITTEE FOR AERONAUTICS

WASHINGTON

JUL 2 1952

NACA RM SL52F20

NATIONAL ADVISORY COMMITTEE FOR AERONAUTICS

RESEARCH MEMORANDUM

for the

Air Materiel Command, U. S. Air Force

AN INVESTIGATION OF THE EFFECT OF THE WADC 30,000-HORSEPOWER WHIRL RIG UPON THE STATIC CHARACTERISTICS OF A PROPELLER

By Leland B. Salters, Jr., and Harry T. Norton, Jr.

SUMMARY

Tests have been made at the Langley Aeronautical Laboratory on a 6000-horsepower propeller dynamometer installed at a ground test facility to determine the effect of a half-scale model of the Wright Aeronautical Development Center 30,000-horsepower whirl rig upon the aerodynamic characteristics of a three-blade NACA 10-(3)(062)-045 propeller. The model of the whirl rig was mounted in front of the 6000-horsepower propeller dynamometer. Static propeller tests were made for 0°, 5°, 10°, 15°, and 20° blade angles over a range of rotational speeds from 600 to 2200 rpm in 100-rpm increments. Measurements were made of propeller thrust and torque, stresses in the propeller blades, and static and total pressures over the surface of the model.

Propeller thrust and torque were increased up to 33 percent by the presence of the model of the whirl rig, but the average increase was from 5 to 10 percent. Blade vibratory stresses were small.

INTRODUCTION

During the design of the 30,000-horsepower propeller whirl rig at the Wright Aeronautical Development Center, the National Advisory Committee for Aeronautics was requested to conduct static propeller tests upon a half-scale model of the proposed whirl rig. It was requested that the half-scale model be tested in conjunction with a 6000-horsepower propeller dynamometer at the Langley Laboratory, using a 10-foot, three-blade propeller.

The proposed 30,000-horsepower whirl rig is of such design as to present a bluff body to the propeller slipstream close to the propeller disk. The primary purpose of the tests was to determine the effects of the whirl-rig interference on propeller aerodynamic characteristics. The secondary purpose of the tests was to obtain the air loads produced upon the motor housing by the propeller slipstream. By statically testing a propeller on the 6000-horsepower propeller dynamometer in the presence of the scale model of the whirl rig, and making similar tests without the model, comparisons may be made to determine the effect of the model upon the aerodynamic characteristics of the propeller.

SYMBOLS

b	blade width, ft
c_{l_d}	design section lift coefficient
C_P	power coefficient, $\frac{P}{\rho n^3 D^5}$
C_T	thrust coefficient, $\frac{T}{\rho n^2 D^4}$
C_T/C_P	static thrust figure of merit
D	propeller diameter, ft
h	blade section maximum thickness, ft
H	total pressure, lb/sq ft
$\frac{\Delta H}{p_a}$	pressure coefficient, $\frac{H - p_a}{p_a}$
M_t	rotational tip Mach number
n	propeller rotational speed, rps
p	static pressure, lb/sq ft
P	power, ft-lb/sec
p_a	atmospheric pressure, lb/sq ft

$\frac{\Delta p}{p_a}$	pressure coefficient, $\frac{p - p_a}{p_a}$
r	propeller radius, ft
R	propeller-tip radius, ft
T	thrust, lb
V_t	rotational tip speed, πnD, ft/sec
β	blade angle, deg
$\beta_{0.75R}$	blade angle at 0.75 tip radius, deg
ρ	air density, slugs/cu ft

APPARATUS

Propeller.- An NACA 10-(3)(062)-045 three-blade propeller was mounted on the rear unit of a 6000-horsepower propeller dynamometer as described in reference 1 and shown in figure 1. Blade-form curves are given in figure 2. For further description of the blades, see references 2 and 3.

Strain-gage installation.- A strain gage was installed on the thrust face of one of the blades at the 18-inch radial station. The wires of the gage were oriented to measure combined bending and centrifugal stresses in the propeller blades. The electrical leads were connected through pineapple-type slip rings on the dynamometer shaft to a recording oscillograph.

Whirl-rig model.- A half-scale model of the front part of the WADC 30,000-horsepower whirl rig was constructed of sheet metal and mounted on an open framework in front of the dynamometer. Figure 3 is a photograph of the model without the gear-box housing and figure 4 is a photograph with the gear-box housing in place. The principal dimensions of the model are given in figure 5.

It was desired to find the effects of the whirl-rig model upon a propeller tested in two locations on the rig. The design of the whirl rig provides for either of two parallel shafts for testing of propellers, the lower shaft for large propellers of low rotational speed and the upper shaft for smaller propellers of higher rotational speeds. In addition, the upper shaft is provided with an extension in the form of

a gear box for increasing propeller rotational speeds. This gear-box extension placed the propeller disk 0.608D (D = 10 ft) away from the face of the whirl-rig model; without the extension the propeller disk was 0.133D away from the face of the model. It was therefore found desirable to determine the effect of the model upon a propeller on the lower shaft close to the front face of the rig and upon a propeller on the upper shaft with the gear-box extension in place.

Pressure measurements.- Static orifices and total-pressure tubes were installed on the model surface at locations requested by the WADC. Orifices of the total-pressure tubes were located 4 inches above the surface. A sketch showing orifice and total-pressure-tube locations and numbers is shown in figure 6. Pressures were measured by means of a liquid manometer and were recorded photographically. The pressure instrumentation was installed to determine the air loads on the structure.

TESTS

The NACA 10-(3)(062)-045 propeller, mounted on the rear unit of the 6000-horsepower propeller dynamometer, was tested statically at blade angles $\beta_{0.75R}$ of 0°, 5°, 10°, 15°, and 20°. Thrust, torque, and blade stresses were measured over a speed range of from 600 to 2200 rpm in increments of 100 rpm for both pusher and tractor arrangements. Tests were made without the whirl-rig model and with the model mounted near the dynamometer in two positions. The six configurations used in these tests are shown in figure 7 and the positioning of the model relative to the dynamometer is shown in figure 8. Total and static pressures were measured for configurations IV and VI. For configurations III and V the pressures were found to be too small to record.

Because of the sensitivity of thrust and torque to wind speed and direction, tests were not made when the wind speed exceeded 5 miles per hour.

RESULTS AND DISCUSSION

Effect of model on thrust and power coefficients.- Curves of thrust coefficient and power coefficient plotted against rotational tip Mach number for tractor configurations II, IV, and VI are given in figure 9 and for pusher configurations I, III, and V in figure 10. The scatter of the test points during a typical run is shown in figure 9 for the blade angle of 10°. This scatter is believed to be caused primarily by small changes in wind velocity and direction, and is more pronounced at low rotational speeds when the over-all measured forces are small.

An examination of the curves of figures 9 and 10 discloses the fact that there was a definite effect upon the propeller performance due to the presence of the model, the effect being more pronounced without the gear-box extension, in which case the bluff body was nearer to the plane of rotation of the propeller. For both pusher and tractor arrangements the presence of the model as in configurations III and IV increased thrust and torque up to 13 percent and as in configurations V and VI increased them up to 33 percent, but the average increase was from 5 to 10 percent. The relative interference effects are shown more clearly by the variation of ΔC_T and ΔC_P with rotational tip Mach number in figures 11 and 12. These increments were obtained by subtracting the coefficients for the configurations without the whirl rig from those with the whirl rig in place.

In figure 13, static thrust figure of merit C_T/C_P is plotted against power coefficient C_P for rotational tip Mach numbers of 0.60 and 0.80 for the tractor configuration. This shows that the ratio C_T/C_P, which is an indication of efficiency for static propeller tests, is not as greatly affected by the presence of the model as the thrust and torque.

The increases in C_T and C_T/C_P due to the presence of the whirl-rig model are attributed to the blockage produced by the model upon the induced-flow field of the propeller. In reference 4 it may be seen that blockage in the form of ground effect greatly increased the C_T and C_T/C_P for the rotor. In the case of incomplete blockage such as that due to the obstruction caused by the whirl-rig model, the effects are similar but smaller in magnitude.

Comparison of results with those of reference 5.- A comparison of the results of these tests with those of reference 5 is shown in figure 14 in which T/D^2 is plotted against rotational tip speed. Figure 14 shows the difference in range covered by the two investigations, and that the interference effects were much greater for the present tests than for the earlier small-scale tests. It should be pointed out that although the whirl-rig models were designed to represent two different whirl rigs, they are fairly similar in shape and are comparable as to scale. From a visual comparison it would appear that the ratio of the size of the obstruction to the size of the propeller is about the same for both investigations.

The comparison made in figure 14 could not be put on a nondimensional basis because reference 5 did not present values of air density, coefficients, nor a description of the propeller. The diameter of the propeller used in the present tests is four times the diameter of the propeller used in reference 5. Also, the plan forms of the two propellers are quite different. The blade width of the propeller of reference 5 is the smaller especially near the tips. From a visual comparison it would

appear that the solidity of the NACA blades is at least twice that of the other. In accord with this difference, the thrust coefficients of the NACA propeller are approximately twice that of the other at equal blade angles. Also, the blade-section Reynolds number of the NACA tests is approximately eight times that of reference 5 for equal tip speeds. The differences in results of the two tests may, therefore, be due to differences in scale and blade design. It should be emphasized here that the interference effects are different for different propellers and that the results of the present investigation are applicable only to the subject propeller and not to propellers in general.

Pressure distribution over model surface.- Pressure coefficients for total and static pressures are presented in tables I and II for representative tests. Table I contains pressure coefficients for configuration IV and table II, for configuration VI. For configurations III and V the pressures were so small they were considered to be negligible.

It may be noticed that the pressures on opposite sides of the model do not agree, which indicates an unsymmetrical flow pattern over the model. (Orifice locations are shown in fig. 4.) During the test runs it was observed that velocities in the wake were much larger on one side of the model than the other. This result has been attributed to the effect of slipstream rotation. Consideration of the static pressures indicates that orifices 8, 12, and 16 have greater values of negative pressure coefficient than for other comparable orifices. This difference is apparently due to the proximity of these tubes to the sharp bend in the model surface. Potential theory would predict such a velocity increase near a sharp corner.

A photograph of the flow about the front end of the model, as indicated by tufts, for configuration VI, $\beta_{0.75R} = 30^\circ$ is shown in figure 3.

Effect of presence of model on propeller blade stresses.- Curves of steady stress and half-amplitude vibratory stress plotted against rotational speed for representative tests are shown in figures 15 and 16. A comparison of these curves indicates an increase in blade steady stresses due to the presence of the model, the magnitude of the increases being of the same order as for thrust and power coefficients. It would therefore appear that the increase in steady stress was due to increased thrust and torque.

In the case of the vibratory stresses the interference effect of the model is not so clearly defined, although it may be seen that, in general, the effect is to increase the vibratory stresses. Near 1200 rpm a resonant condition becomes noticeable, especially for the tractor configurations. This resonance becomes large enough to overshadow other influences near 1200 rpm, and reaches a maximum for $\beta_{0.75R} = 20^\circ$ (fig. 15(c)). The

maximum stress in this case occurs without the presence of the model, the effect of the model being to dampen the vibrations. The fact that the maximum vibratory stress occurs without the model seems to indicate that it is caused by the NACA dynamometer and not by the model.

CONCLUDING REMARKS

Static propeller tests to determine the effect of the WADC 30,000-horsepower whirl rig upon the aerodynamic characteristics of a three-blade NACA 10-(3)(062)-045 propeller showed important effects:

The presence of the whirl-rig model increased the propeller thrust and torque as much as 13 percent for the widely separated configuration (propeller disk to body face distance = 0.61D) and as much as 33 percent for the closely spaced configuration (propeller disk to body face distance = 0.13D); however, the average increase was from 5 to 10 percent. On the other hand the ratio of thrust coefficient to power coefficient was little affected by the proximity of the whirl-rig model and the propeller.

The increase in the propeller blade steady stresses due to the presence of the model was of the same order as the increases in propeller thrust and torque. The vibratory stresses in the propeller were generally increased by the presence of the body, but for the propeller used the vibratory stresses were always small.

Langley Aeronautical Laboratory
National Advisory Committee for Aeronautics
Langley Field, Va.

Leland B. Salters, Jr.
Leland B. Salters, Jr.
Aeronautical Research Scientist

Harry T. Norton Jr.
Harry T. Norton, Jr.
Aeronautical Research Scientist

Approved: Eugene C. Draley
Eugene C. Draley
Chief of Full-Scale Research Division

JLC

[redacted]

REFERENCES

1. Wood, John H., and Swihart, John M.: The Effect of Blade-Section Camber on the Static Characteristics of Three NACA Propellers. NACA RM L51L28, 1952.

2. Soloman, William: Aerodynamic Characteristics at High Speeds of a Two-Blade NACA 10-(3)(062)-045 Propeller and of a Two-Blade NACA 10-(3)(08)-045 Propeller. NACA RM L8E26, 1948.

3. Shaw, Alex E.: Whirl Test of Hartman Design Propeller Blades for Use in Aerodynamic Testing in Wind Tunnel at Langley Field, Virginia. Whirl Test No. 1788. AAF TR No. 5007. Materiel Center, Army Air Forces, Sept. 2, 1943.

4. Knight, Montgomery, and Hefner, Ralph A.: Analysis of Ground Effect on the Lifting Airscrew. NACA TN 835, 1941.

5. Jacobs, H. H., and Loedding, A. C.: Test of 1/4 Scale Model No. 3 Propeller Whirl Rig in Connection With 5-Foot Wind Tunnel Propeller Balance. Test No. 207. ACTR No. 4461, Materiel Div., Army Air Corps, June 12, 1939.

TABLE I.- PRESSURE DISTRIBUTION OVER MODEL SURFACE FOR CONFIGURATION IV (TRACTOR, NOSE EXTENSION)

Propeller speed (rpm)	Pressure coefficient																			
	$\frac{\Delta H}{p_a} \times 10^4$				$\frac{\Delta p}{p_a} \times 10^4$															
	Tube number				Orifice number															
	1	2	3	4	5	6	7	8	9	10	11	12	13	14	15	16	17	18	19	20
$\beta_{0.75R} = 0°$																				
599.5	6	6	4	4	0	0	0	-2	0	0	0	-2	0	0	0	-2	0	0	0	0
800	12	12	10	7	0	0	0	-3	0	0	0	-4	0	0	0	-4	0	0	0	0
1000	20	20	16	12	0	0	0	-4	0	0	-1	-4	0	0	0	-6	0	0	0	0
1151	28	27	20	16	0	0	0	-6	0	0	-2	-4	0	0	0	-6	0	0	0	0
1250	34	33	26	22	0	0	0	-6	0	0	-2	-6	0	0	0	-8	0	0	0	0
1400	41	42	34	26	0	0	0	-6	0	0	-2	-8	0	0	0	-10	0	0	0	0
1603	53	55	44	32	0	0	1	-8	0	0	-3	-10	0	0	0	-14	0	0	0	0
1800	69	73	55	42	2	0	1	-10	0	0	-4	-12	0	0	-1	-18	0	0	1	1
2000	81	90	67	51	3	0	2	-12	0	0	-4	-16	0	0	-1	-22	0	1	2	1
2215	111	113	93	71	4	0	2	-16	0	0	-2	-18	0	0	-1	-26	0	1	2	2
2101	99	104	88	70	2	0	3	-13	0	0	-2	-15	0	0	-1	-23	0	1	2	1
1900	87	81	61	48	1	0	2	-12	0	0	-1	-12	0	0	0	-18	0	0	1	1
1700	64	66	52	41	0	0	1	-9	0	0	-1	-10	0	0	0	-15	0	0	0	0
1499	51	51	42	36	0	0	0	-10	0	0	-1	-8	0	0	0	-10	0	0	0	0
1298.5	38	38	31	24	0	0	0	-6	0	0	0	-6	0	0	0	-8	0	0	0	0
1100	26	25	20	18	0	0	0	-6	0	0	0	-4	0	0	0	-6	0	0	0	0
900	16	16	10	8	0	0	0	-4	0	0	0	-2	0	0	0	-4	0	0	0	0
702.5	10	9	6	6	0	0	0	-3	0	0	0	-2	0	0	0	-2	0	0	0	0
598	6	6	4	2	0	0	0	-2	0	0	0	-2	0	0	0	-2	0	0	0	0
$\beta_{0.75R} = 15°$																				
600	18	20	16	16	0	0	1	-4	0	0	-2	-4	0	0	0	-4	0	0	1	0
800.5	32	32	28	22	-2	0	1	-6	0	0	-4	-8	-1	0	-1	-8	0	0	2	1
1000	53	53	45	39	-1	0	3	-8	0	0	-4	-12	-1	-1	-1	-16	-1	0	2	1
1150	65	75	66	59	2	0	2	-14	0	0	-4	-16	-2	-1	0	-22	-1	0	3	2
1253	87	89	83	73	2	0	3	-16	0	0	-4	-16	-2	-1	0	-28	-1	0	4	2
1401	95	101	97	107	3	0	2	-22	0	-1	-5	-22	-2	-2	0	-35	-2	1	7	3
1600	132	132	122	111	3	0	5	-28	0	-2	-5	-32	-3	-2	0	-47	-2	1	10	4
1806	170	176	158	146	7	0	7	-36	0	-2	-6	-37	4	-2	0	-59	-2	2	12	7
2000	217	227	209	195	6	0	0	-45	0	-3	-6	-48	4	-3	4	-79	-4	3	16	10
2205	247	270	245	223	-2	0	6	-57	0	-2	-4	-62	-5	-5	5	-99	-3	3	22	13
2100	229	245	225	207	14	0	-2	-47	0	-3	-6	-55	-4	-3	2	-91	-3	3	20	11
1896.5	174	203	189	176	3	0	3	-39	0	-3	-4	-39	-2	-3	3	-67	-3	3	13	8
1702	154	162	150	140	5	0	3	-36	0	-4	-2	-36	-1	-1	1	-55	-1	3	9	5
1500	111	140	128	99	5	0	3	-23	0	-2	-6	-24	-3	-2	-3	-40	-1	2	11	3
1300	89	95	89	75	2	0	3	-16	0	-1	-3	-18	-2	0	0	-28	-1	1	7	3
1103	64	72	62	51	1	0	3	-11	0	0	-3	-13	-2	0	-1	-21	-1	0	4	2
899	41	47	45	41	1	0	1	-10	0	0	-1	-10	0	0	0	-10	0	0	2	1
700	30	31	27	23	1	0	1	-5	0	0	-1	-5	0	0	0	-6	0	0	1	0
596.5	19	20	17	16	0	0	1	-5	0	0	-1	-4	0	0	0	-4	0	0	1	0
$\beta_{0.75R} = 20°$																				
598	18	18	17	---	-1	0	0	-6	0	0	-4	-6	-2	0	0	-9	0	0	1	0
800	32	40	38	---	-2	0	-1	-7	0	0	-4	-10	-2	-1	0	-14	0	0	2	1
1000	46	61	57	---	-8	0	-2	-10	0	0	-6	-16	-3	-1	0	-22	-1	0	4	2
1150	58	54	53	---	-5	0	-3	-11	0	0	-9	-21	-3	-2	0	-29	-1	0	7	3
1250	70	93	93	---	-12	0	-4	-18	0	0	-10	-26	-3	-4	0	-31	-1	1	8	5
1400	92	98	92	---	-19	0	-9	-21	0	-1	-15	-36	-7	-4	0	-47	-3	1	11	5
1600	105	142	140	---	-28	0	-16	-26	0	-1	-19	-45	-8	-6	0	-59	-5	1	14	7
1800	143	155	151	---	-33	0	-19	-31	0	-2	-21	-58	-7	-6	0	-71	-5	3	17	8
2000	168	202	204	---	-40	0	-20	-40	0	-2	-24	-69	-10	-7	0	-88	-6	4	24	11
1900	162	176	169	---	-38	0	-26	-32	0	-4	-22	-63	-8	-7	0	-79	-4	3	22	11
1702.5	133	145	138	---	-30	0	-17	-27	0	-3	-27	-56	-11	-7	0	-70	-4	2	17	8
1499	91	109	106	---	-15	0	-6	-24	0	-2	-19	-42	-8	-6	0	-53	-4	1	10	6
1300	76	84	84	---	-13	0	-6	-18	0	-1	-12	-31	-6	-4	0	-38	-3	0	8	4
1100	53	61	63	---	-8	0	-1	-14	0	0	-9	-22	-6	-2	0	-28	-2	0	6	2
900	45	47	43	---	-4	0	0	-10	0	0	-5	-14	-2	-1	0	-18	-1	0	4	2
700	32	27	25	---	-3	0	0	-7	0	0	-3	-9	-1	-1	0	-11	0	0	1	1
600	32	22	18	---	-2	0	0	-4	0	0	-2	-5	0	0	0	-7	0	0	1	1
$\beta_{0.75R} = 30°$																				
599	20	19	14	---	-8	0	-8	-4	0	0	-5	-7	-3	0	0	-10	-1	-1	2	1
800	25	32	20	---	-13	0	-14	-5	0	-1	-10	-10	-4	0	-1	-18	-2	-1	6	2
999	47	49	34	---	-23	0	-24	-7	0	-1	-16	-20	-6	-1	-3	-30	-5	-2	8	2
1148	60	72	49	---	-29	0	-27	-9	0	-2	-19	-25	-6	-2	-4	-33	-5	-2	9	3
1100	59	56	32	---	-22	0	-24	-8	0	-1	-20	-22	-6	-2	-4	-36	-6	-3	8	4
898.5	45	40	24	---	-16	0	-18	-6	0	-1	-14	-16	-6	-1	-3	-24	-4	-2	6	2
702	34	26	14	---	-11	0	-10	-4	0	-1	-8	-10	-4	-1	-1	-14	-2	-2	4	2
600	30	18	10	---	-6	0	-8	-4	0	0	-4	-6	-3	0	-1	-12	-2	-1	2	1

TABLE II.- PRESSURE DISTRIBUTION OVER MODEL SURFACE FOR CONFIGURATION VI (TRACTOR)

Propeller speed (rpm)	Pressure coefficient																			
	$\frac{\Delta H}{p_a} \times 10^4$				$\frac{\Delta p}{p_a} \times 10^4$															
	Tube number				Orifice number															
	1	2	3	4	5	6	7	8	9	10	11	12	13	14	15	16	17	18	19	20
$\beta_{0.75R} = 0^\circ$																				
597	5	4	2	2	0	0	0	-1	0	0	0	0	0	0	0	-1	0	0	0	0
800.5	10	8	6	5	0	0	0	-2	0	0	-1	-1	0	0	0	-2	0	0	1	1
1000	16	12	8	7	1	0	0	-3	0	0	-1	-2	0	0	0	-4	0	0	1	1
1149.5	22	17	12	10	1	0	0	-4	0	0	-1	-2	0	0	0	-5	0	0	1	1
1250.5	24	21	15	12	3	0	0	-5	0	0	-2	-3	0	0	0	-6	0	0	1	1
1400	34	29	20	15	2	0	1	-6	0	0	-2	-4	0	0	0	-8	0	0	2	2
1601.5	43	36	25	19	5	0	1	-7	0	0	-3	-6	0	0	0	-10	0	0	2	2
2000	71	57	41	35	6	0	2	-11	0	0	-3	-9	0	0	0	-17	0	1	3	3
2210	89	75	51	41	3	0	2	-12	0	0	-4	-10	0	0	0	-21	0	2	5	4
2100	81	70	50	38	6	0	2	-12	0	0	-4	-9	0	0	0	-19	0	1	3	3
1900	61	51	36	30	7	0	2	-10	0	0	-3	-8	0	0	0	-15	0	1	3	3
1700	44	39	30	22	3	0	2	-8	0	0	-2	-6	0	0	0	-12	0	1	2	2
1500	36	27	20	17	3	0	1	-7	0	0	-2	-4	0	0	0	-9	0	0	2	2
$\beta_{0.75R} = 5^\circ$																				
600	11	9	7	6	0	0	0	-3	0	0	-1	-2	0	0	0	-2	0	0	1	1
800	21	15	9	7	2	0	0	-4	0	0	-1	-2	0	0	0	-4	0	0	1	1
1001.5	33	25	17	15	2	0	0	-6	0	0	-1	-4	0	0	0	-8	0	0	1	2
1150	44	34	25	21	2	0	0	-8	0	0	-2	-6	0	0	0	-11	0	0	2	2
1250	46	44	34	27	4	0	2	-8	0	0	-2	-7	0	0	1	-13	0	0	2	2
1402.5	60	55	42	36	4	0	2	-10	0	0	-2	-8	0	0	1	-16	0	0	2	2
1600	81	73	56	45	7	1	3	-13	1	-1	-2	-11	0	0	2	-21	0	1	3	3
2000	125	104	75	63	13	1	1	-20	1	-2	-1	-15	0	0	2	-34	0	3	7	6
2200	157	144	115	96	9	1	7	-24	2	-3	-1	-20	0	0	4	-40	0	3	10	7
2100	163	132	97	75	11	1	3	-23	1	2	-1	-17	0	0	4	-36	0	4	8	7
1900	113	105	81	68	11	1	5	-18	0	-1	-1	-14	0	0	2	-29	0	3	5	5
1700	96	85	65	50	7	1	3	-14	0	-1	-2	-11	0	0	2	-24	0	1	4	3
1500	68	61	45	39	6	0	4	-11	0	0	-2	-8	0	0	2	-18	0	0	4	3
1300	55	43	44	26	6	0	2	-9	0	0	-2	-6	0	0	2	-12	0	0	2	1
1100	36	33	23	21	3	0	2	-7	0	0	-1	-5	0	0	1	-9	0	0	2	2
901	25	23	17	14	3	0	2	-5	0	0	-1	-3	0	0	1	-6	0	0	1	1
696	16	14	10	8	0	0	0	-3	0	0	-1	-2	0	0	0	-3	0	0	1	1
599	12	9	7	6	0	0	0	-3	0	0	-1	-2	0	0	0	-3	0	0	0	0
$\beta_{0.75R} = 10^\circ$																				
600	18	15	11	10	1	0	1	-1	0	0	0	-2	0	0	1	-4	0	0	0	0
800	30	26	22	16	2	0	0	-6	0	-1	0	-4	0	0	1	-8	0	0	1	1
999	46	42	33	28	2	0	-1	-8	0	-1	-1	-8	0	0	2	-12	0	0	2	1
1150	62	56	43	37	2	0	2	-12	0	-1	-1	-9	0	0	2	-17	0	1	2	1
1251.5	79	67	48	41	4	0	-3	-15	0	-2	-1	-10	0	0	3	-20	0	1	3	1
1400	99	87	68	55	6	0	-1	-18	0	-2	-1	-14	1	0	4	-25	0	2	4	2
1600	134	114	85	70	3	0	-4	-19	1	-3	0	-17	1	0	5	-34	0	2	6	3
2000	207	188	152	133	12	0	-1	-35	1	-3	1	-27	2	-1	11	-53	0	3	12	6
2200	260	237	190	163	19	1	1	-40	1	-4	3	-35	3	-1	15	-64	-1	4	20	9
2100	227	214	171	151	14	1	-1	-39	1	-3	2	-29	1	-2	12	-57	0	4	16	8
1900	198	167	122	99	-3	1	-6	-28	0	-3	2	-20	2	0	11	-47	0	3	12	6
1700	169	134	95	73	-3	1	-5	-25	0	-3	0	-14	1	0	9	-36	0	3	7	4
1498.5	119	102	77	54	0	1	-4	-17	0	-3	1	-12	1	0	5	-27	0	2	6	3
1298	79	75	61	51	2	0	1	-12	0	-1	0	-11	1	0	3	-22	0	2	4	2
1100	60	49	36	30	1	0	-3	-8	0	0	0	-6	0	0	2	-15	0	1	3	1
899.5	36	34	27	22	1	0	1	-6	0	0	0	-5	0	0	1	-9	0	1	1	1
694	22	20	16	13	1	0	1	-5	0	-1	0	-4	0	0	1	-6	0	0	1	0
595.5	19	17	12	10	1	0	1	-3	0	0	0	-1	0	0	1	-4	0	0	0	0

TABLE II.- PRESSURE DISTRIBUTION OVER MODEL SURFACE FOR CONFIGURATION VI (TRACTOR) - Concluded

Propeller speed (rpm)	Pressure coefficient																			
	$\frac{\Delta H}{p_a} \times 10^4$				$\frac{\Delta p}{p_a} \times 10^4$															
	Tube number				Orifice number															
	1	2	3	4	5	6	7	8	9	10	11	12	13	14	15	16	17	18	19	20
$\beta_{0.75R} = 15^\circ$																				
600	24	20	16	13	-2	0	0	-4	0	-1	0	-3	0	0	2	-5	0	0	2	0
800	42	38	29	23	-3	0	0	-8	0	-1	0	-6	0	0	2	-10	0	0	2	2
1000	69	59	45	37	-5	0	-1	-11	0	-1	0	-10	0	0	3	-19	0	0	4	2
1150	92	81	56	45	-8	0	-2	-14	-1	-2	0	-11	0	0	4	-22	0	1	4	2
1248.5	107	95	76	64	-8	0	0	-16	-1	-2	0	-14	0	0	5	-27	0	1	7	3
1400	142	122	91	70	-13	0	0	-21	-2	-3	0	-17	1	0	8	-35	0	3	9	5
1600	186	160	118	95	-14	0	-4	-25	-2	-3	2	-21	1	0	12	-44	0	4	13	6
2000	309	277	199	161	-28	0	-7	-37	-4	-4	5	-36	4	0	21	-75	0	3	24	12
2187.5	385	326	243	207	-27	0	-8	-50	-3	-5	9	-42	5	0	27	-90	0	7	33	14
2100	359	310	229	187	-35	0	0	-45	-3	-5	11	-39	4	0	27	-81	0	6	29	14
1900	268	239	186	149	-29	0	-4	-34	-3	-5	6	-33	1	0	16	-65	0	5	21	10
1700	216	189	139	108	-21	0	0	-28	-2	-4	4	-23	2	0	13	-50	0	4	13	7
1500	161	141	111	89	-18	0	-3	-22	-2	-3	3	-19	1	0	7	-39	0	2	10	6
1301.5	116	100	77	68	-8	0	-1	-15	-1	-2	2	-13	0	0	7	-29	0	1	8	5
1100	81	71	54	45	-5	0	0	-12	-1	-2	1	-10	0	0	4	-20	0	1	4	3
901.5	57	50	37	29	-5	0	0	-9	-1	-2	1	-9	0	0	2	-14	0	0	3	2
700	35	28	19	15	-3	0	0	-6	0	-1	0	-4	0	0	2	-8	0	0	2	0
600	23	22	16	12	-2	0	1	-4	0	-1	0	-4	0	0	0	-6	0	0	1	0
$\beta_{0.75R} = 20^\circ$																				
1000	94	79	52	40	-10	0	-7	-11	0	-2	-1	-12	0	0	1	-22	-1	1	5	3
1153.5	122	103	67	53	-14	0	-8	-13	-1	-2	-2	-14	0	0	3	-28	-1	1	7	5
1254	145	119	78	58	-19	0	-11	-15	-1	-2	-3	-16	0	0	3	-35	-1	1	35	5
1400	185	150	103	83	-25	0	-14	-16	2	-2	-4	-19	0	0	4	-42	-2	2	12	7
1600.5	242	191	124	101	-34	0	-14	-22	2	-2	-4	-26	1	0	4	-57	-2	2	13	7
2000	389	315	191	150	-49	0	-26	-34	-3	-4	-10	-41	2	0	6	-95	-5	2	26	12
1896	361	273	164	125	-47	0	-30	-30	-3	-3	-8	-33	2	0	4	-83	-2	4	24	12
1700	275	223	142	114	-36	0	-18	-26	-2	-4	-5	-27	2	0	3	-65	-2	4	19	11
1500	211	175	111	86	-29	0	-19	-20	-1	-3	-3	-21	1	0	3	-48	-1	3	14	7
1300	158	128	84	66	-21	0	-13	-15	-1	-2	-3	-17	1	0	3	-36	-1	1	11	5
1097.5	113	102	59	45	-15	0	-9	-12	0	-1	-1	-12	0	0	3	-26	-1	1	8	5
896.5	76	62	38	31	-7	0	-5	-8	0	-1	-1	-7	0	0	3	-17	1	1	5	4
699	43	36	22	18	-6	0	-4	7	0	-1	-1	-4	0	0	1	-11	0	0	2	2

Figure 1.- The 6000-horsepower propeller dynamometer without model.
Configuration II.

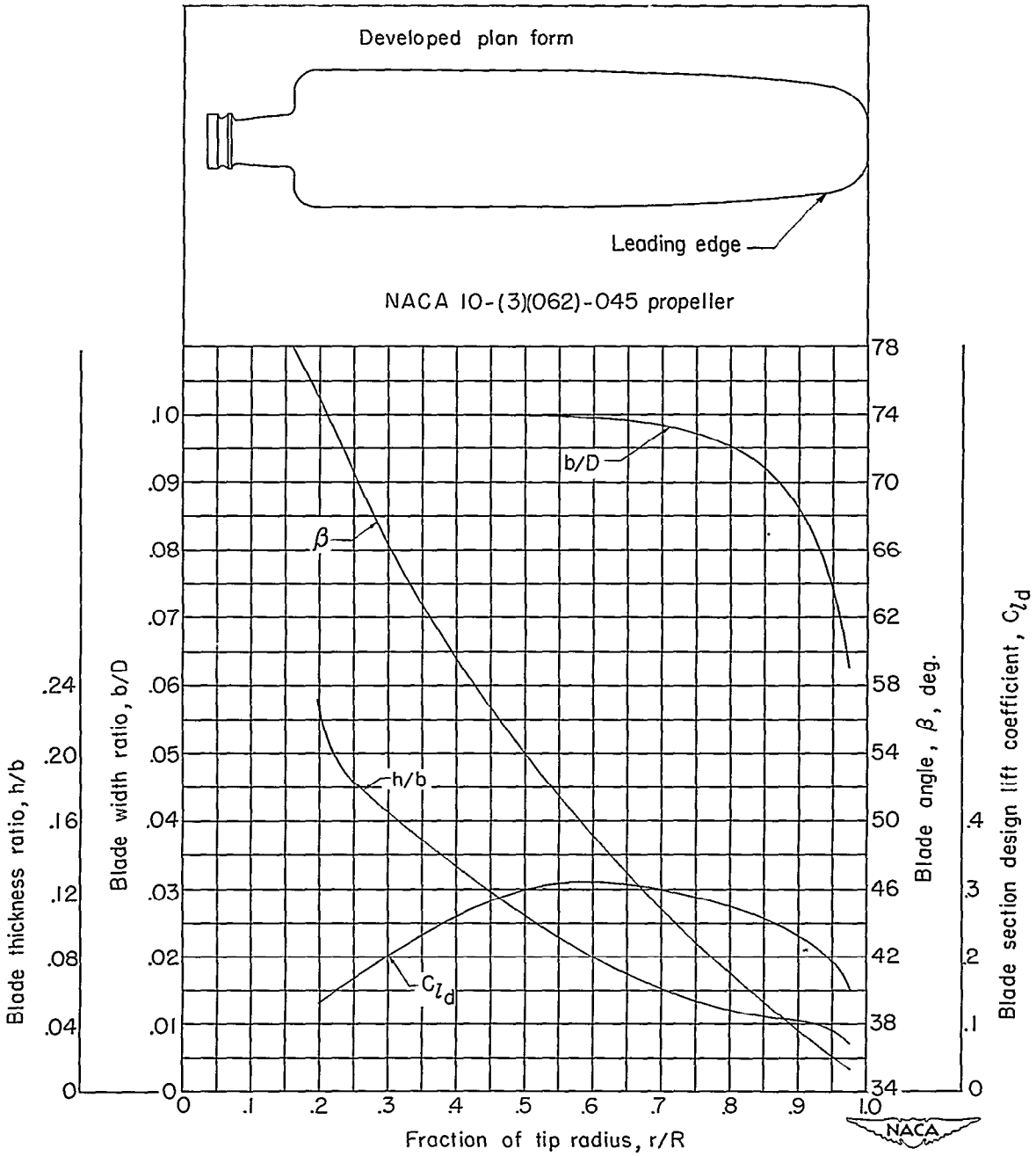

Figure 2.- Blade-form curves for NACA 10-(3)(062)-045 propeller.

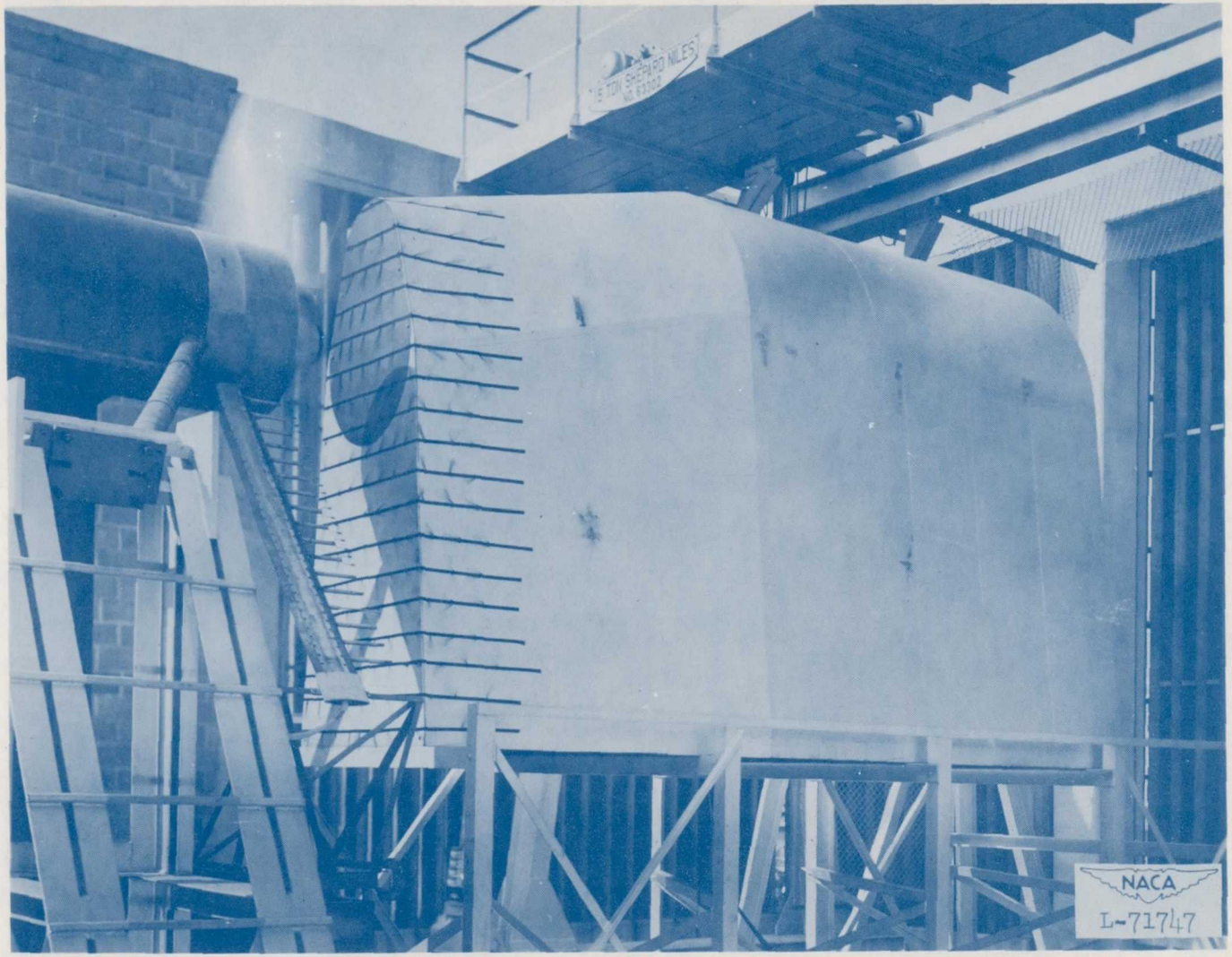

Figure 3.- Dynamometer with model of WADC 30,000-horsepower whirl rig without gear-box housing. Configuration VI.

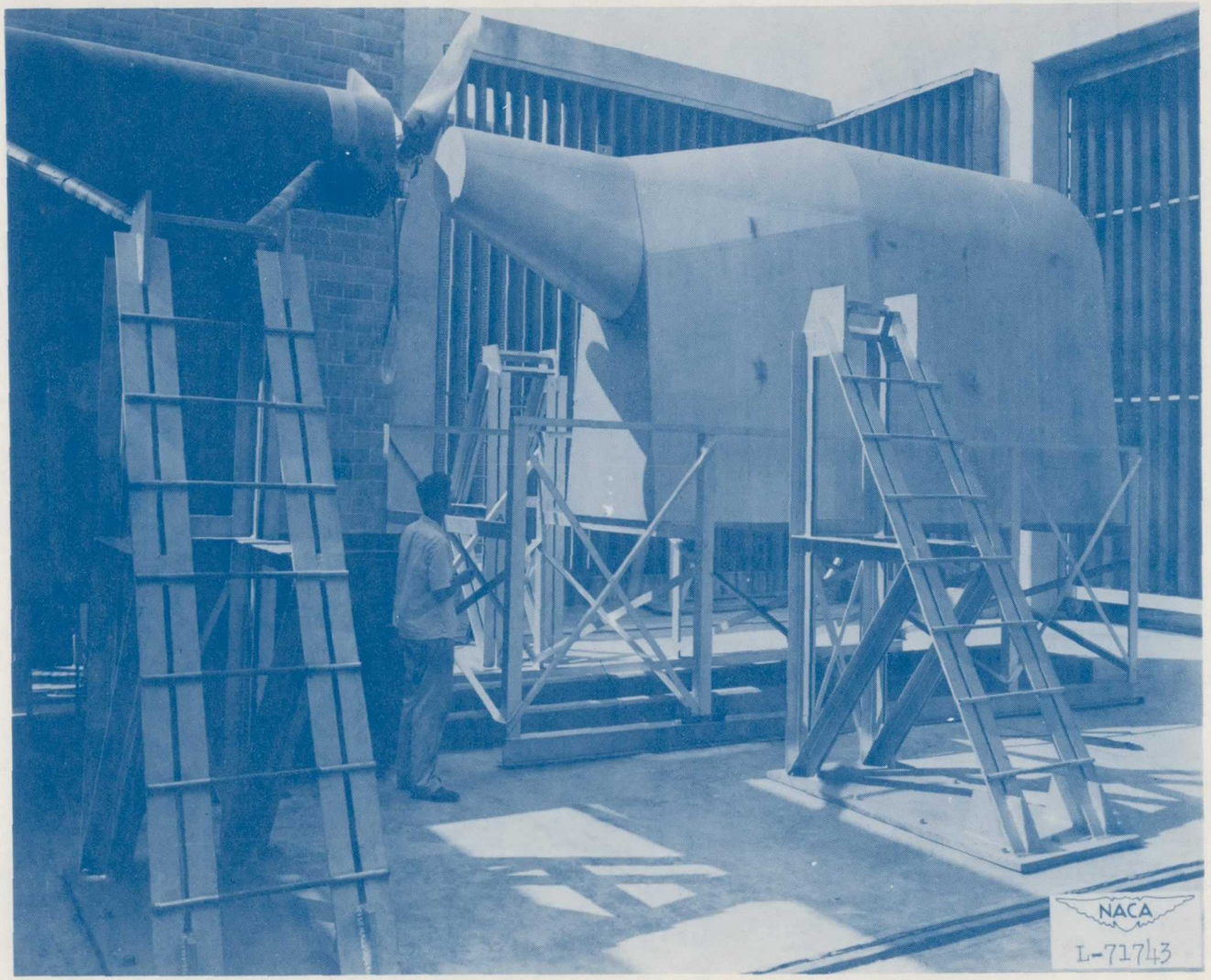

Figure 4.- Dynamometer with model of WADC 30,000-horsepower whirl rig with gear-box housing. Configuration IV.

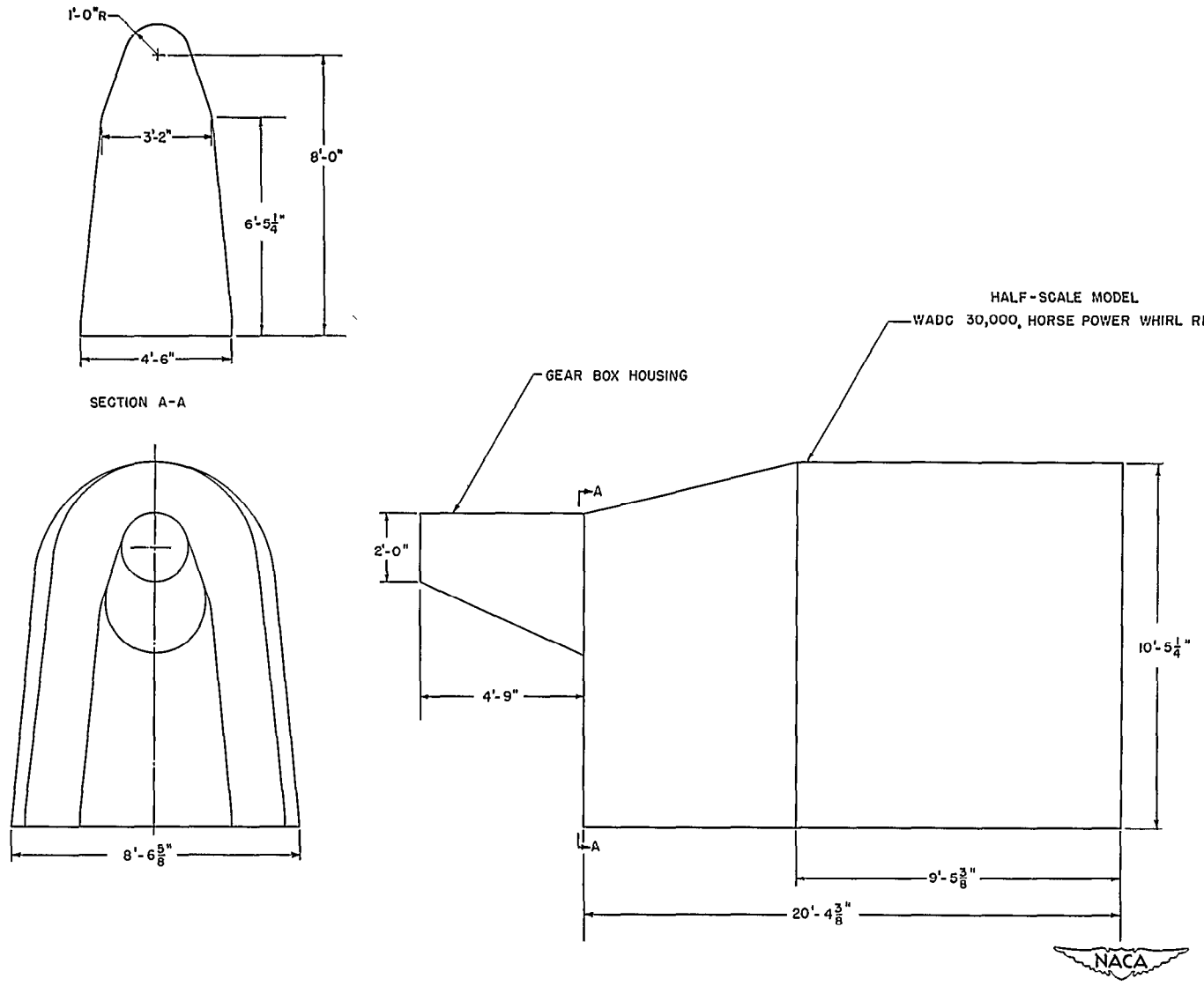

Figure 5.- Half-scale model of the WADC 30,000-horsepower whirl rig with gear-box housing.

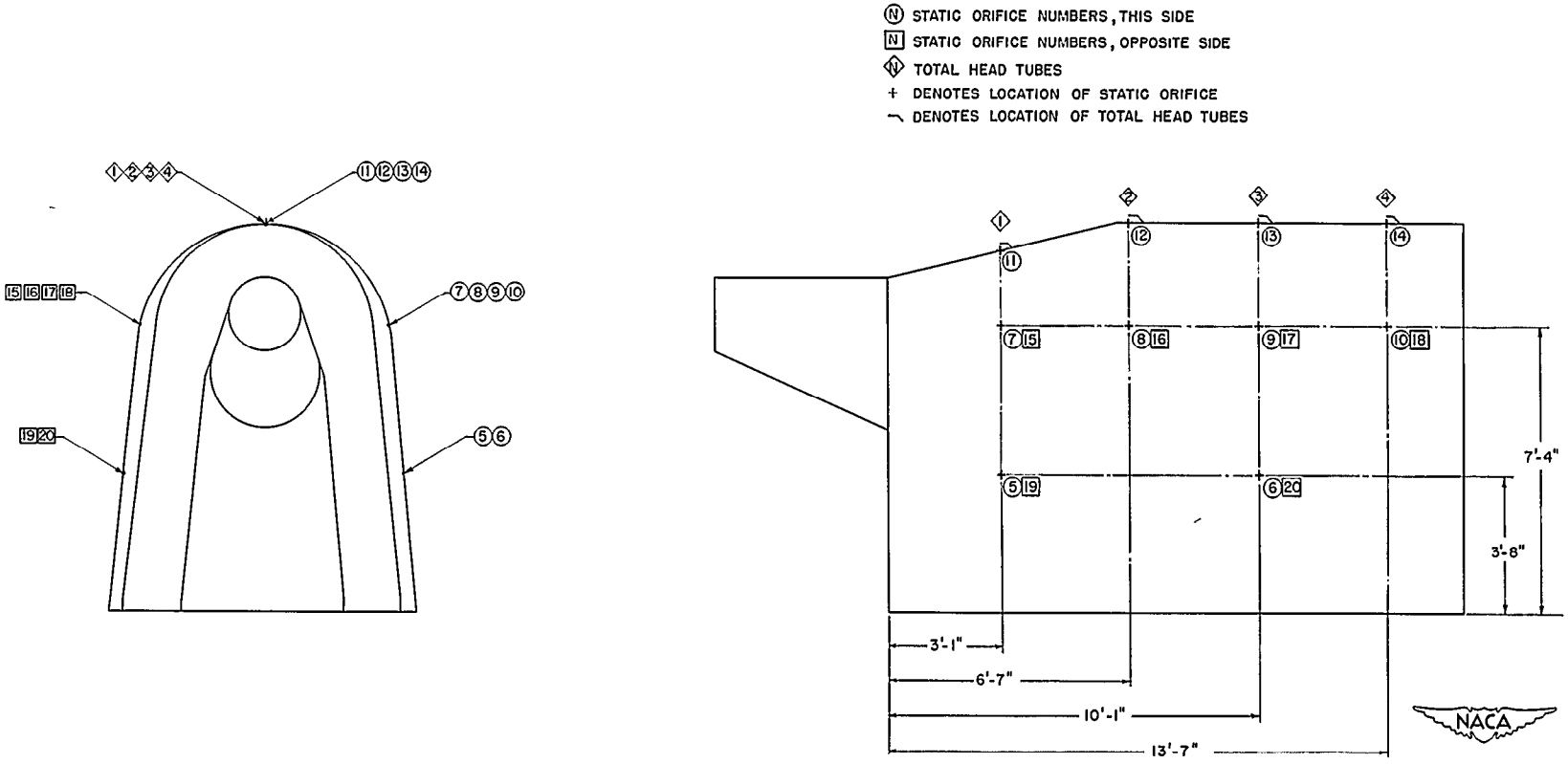

Figure 6.- Location of total head tubes and orifices on surface of model.

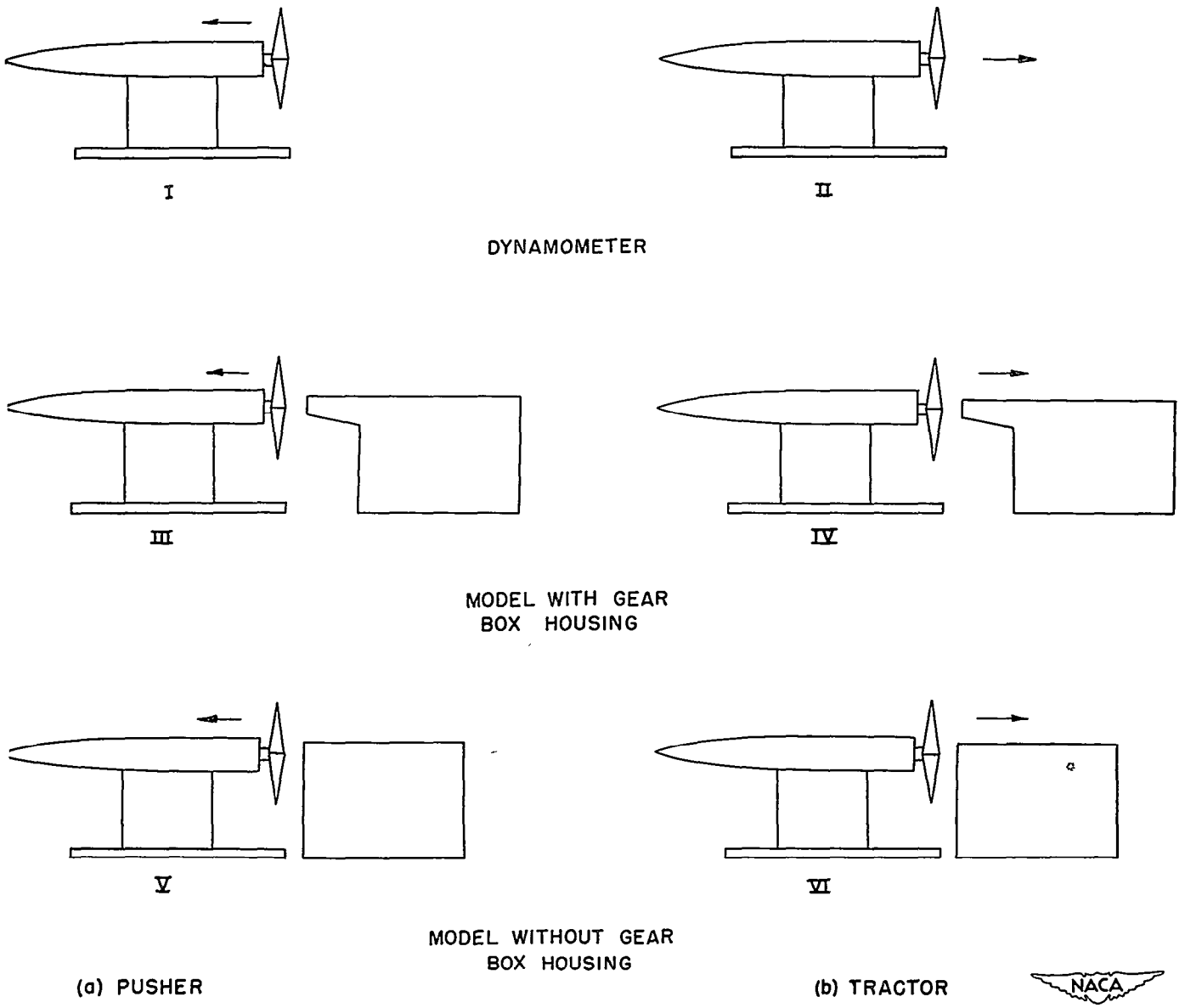

Figure 7.- Test configurations. Arrows indicate direction of slipstream.

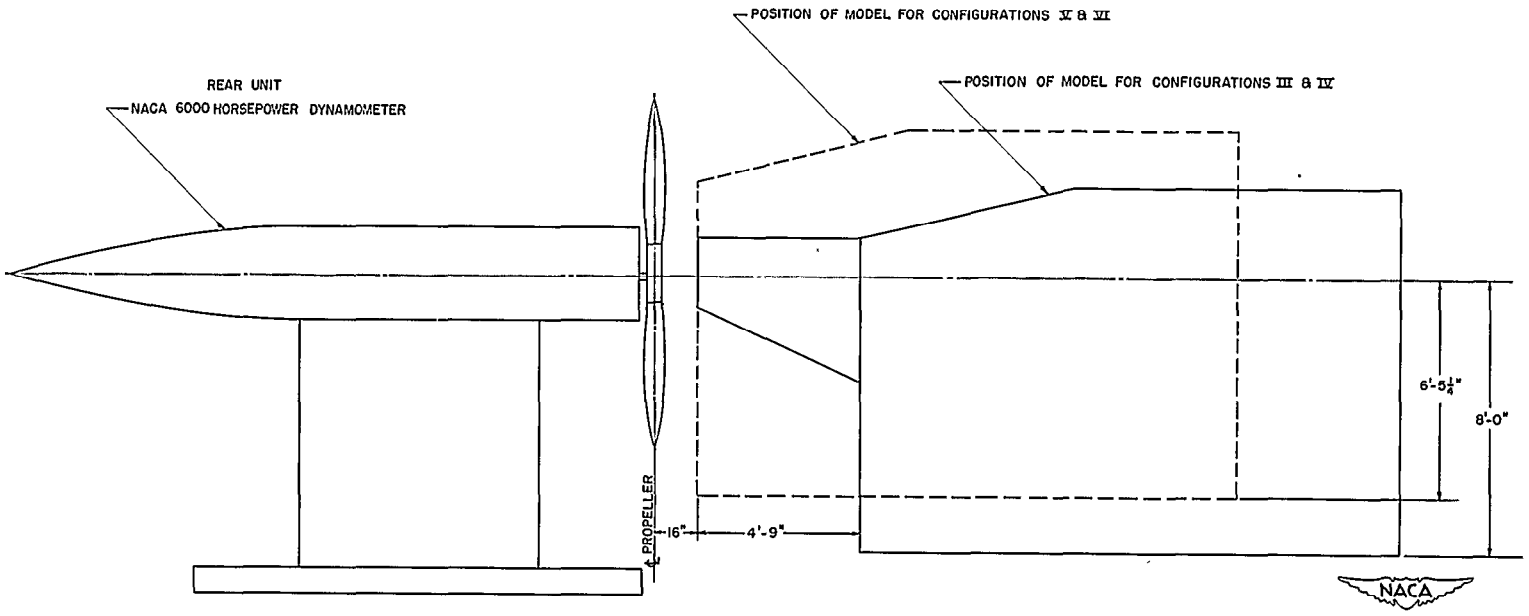

Figure 8.- Positions of model relative to the dynamometer.

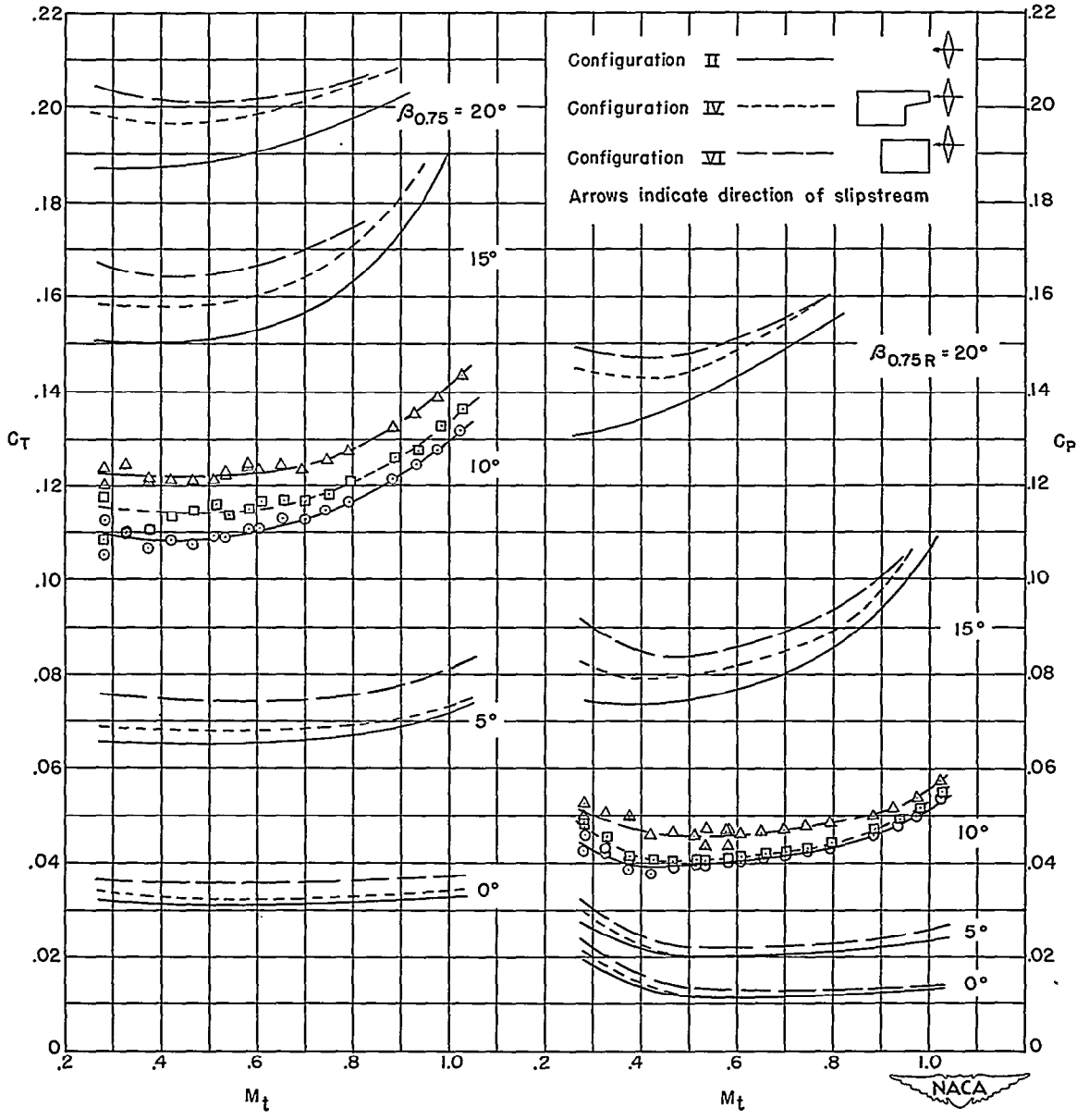

Figure 9.- Variation of static thrust and torque with rotational tip Mach number for tractor configurations.

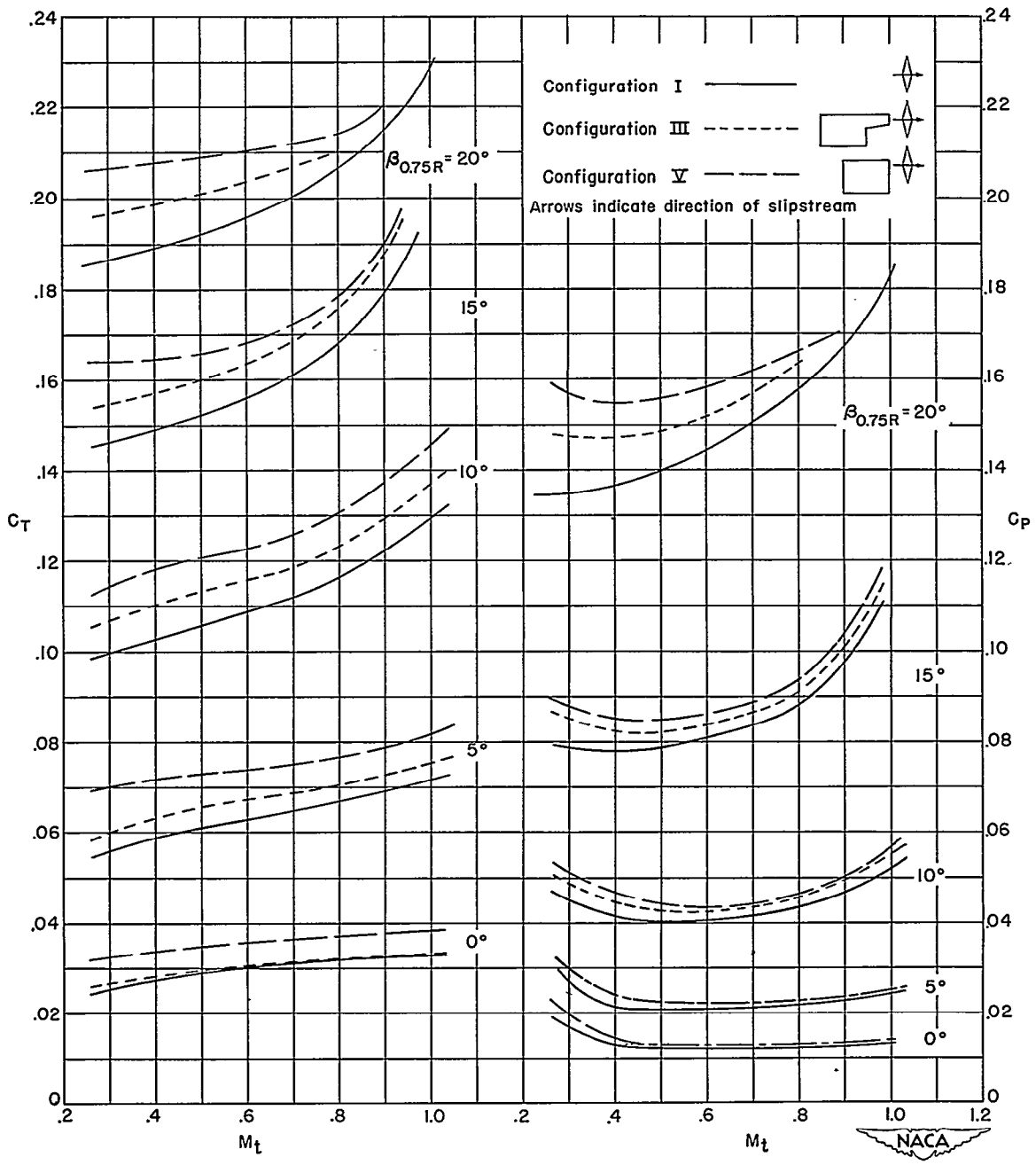

Figure 10.- Variation of static thrust and torque with rotational tip Mach number for pusher configurations.

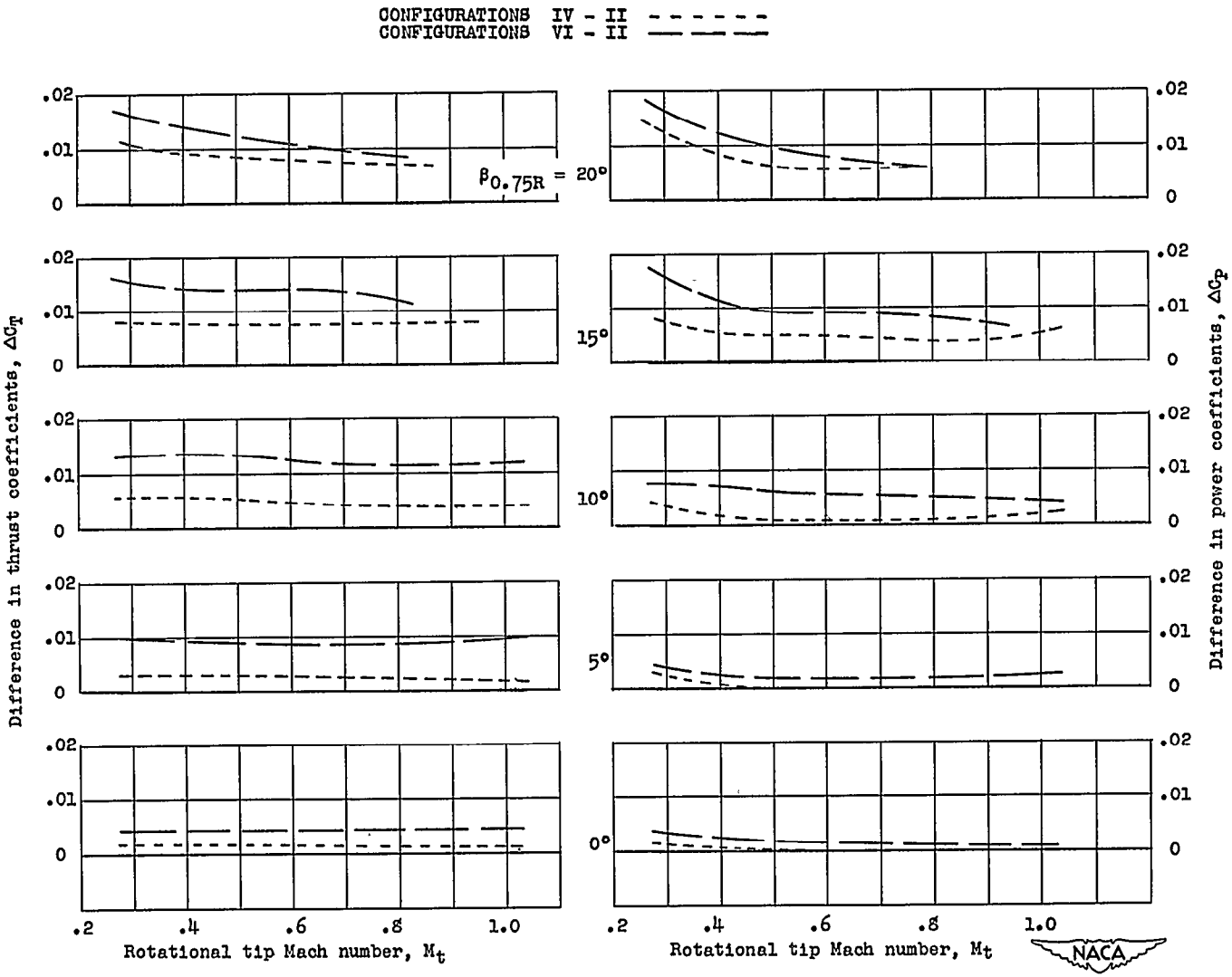

Figure 11.- Variation of ΔC_T and ΔC_P with rotational tip Mach numbers for the tractor configurations.

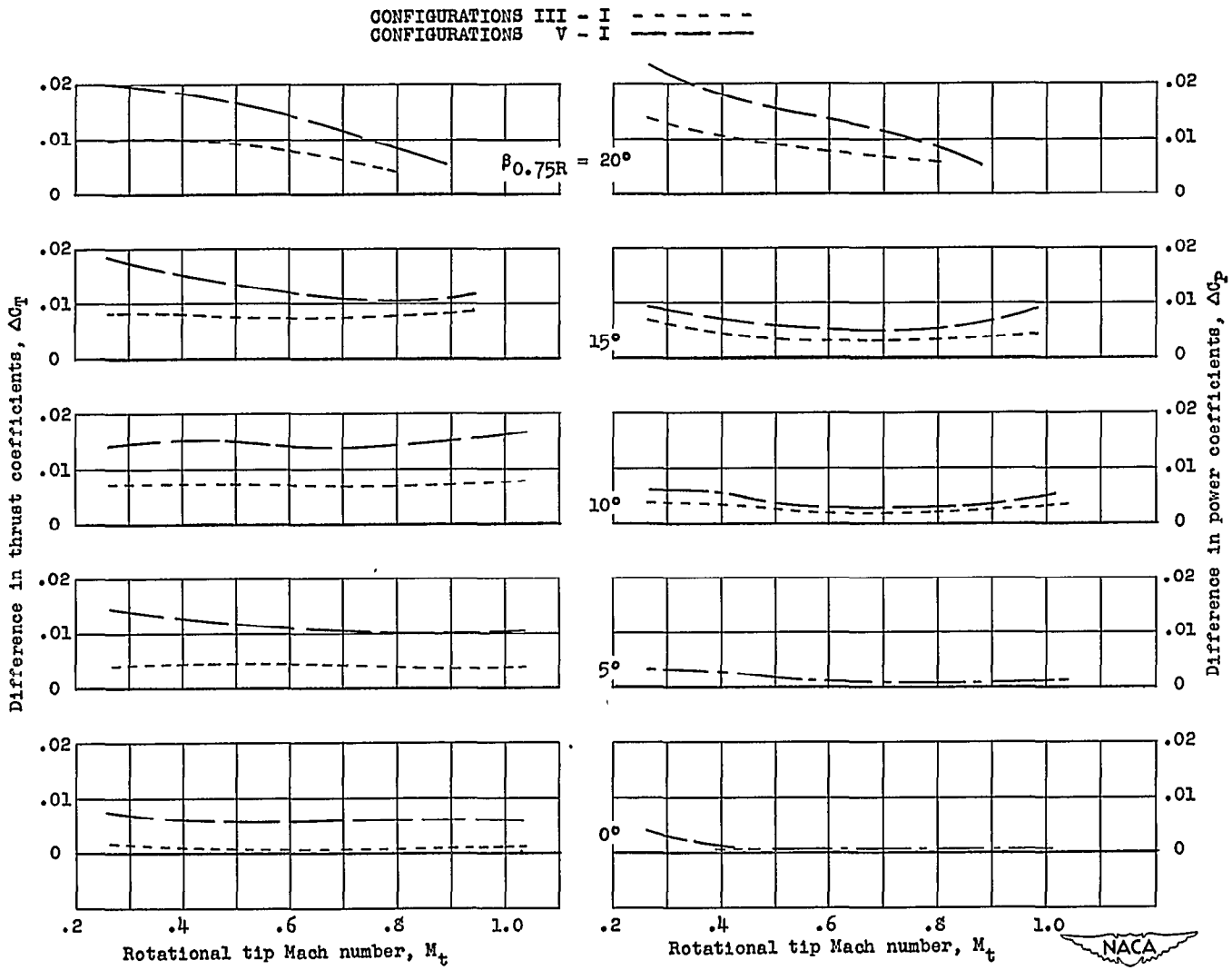

Figure 12.- Variation of ΔC_T and ΔC_P with rotational tip Mach number for the pusher configurations.

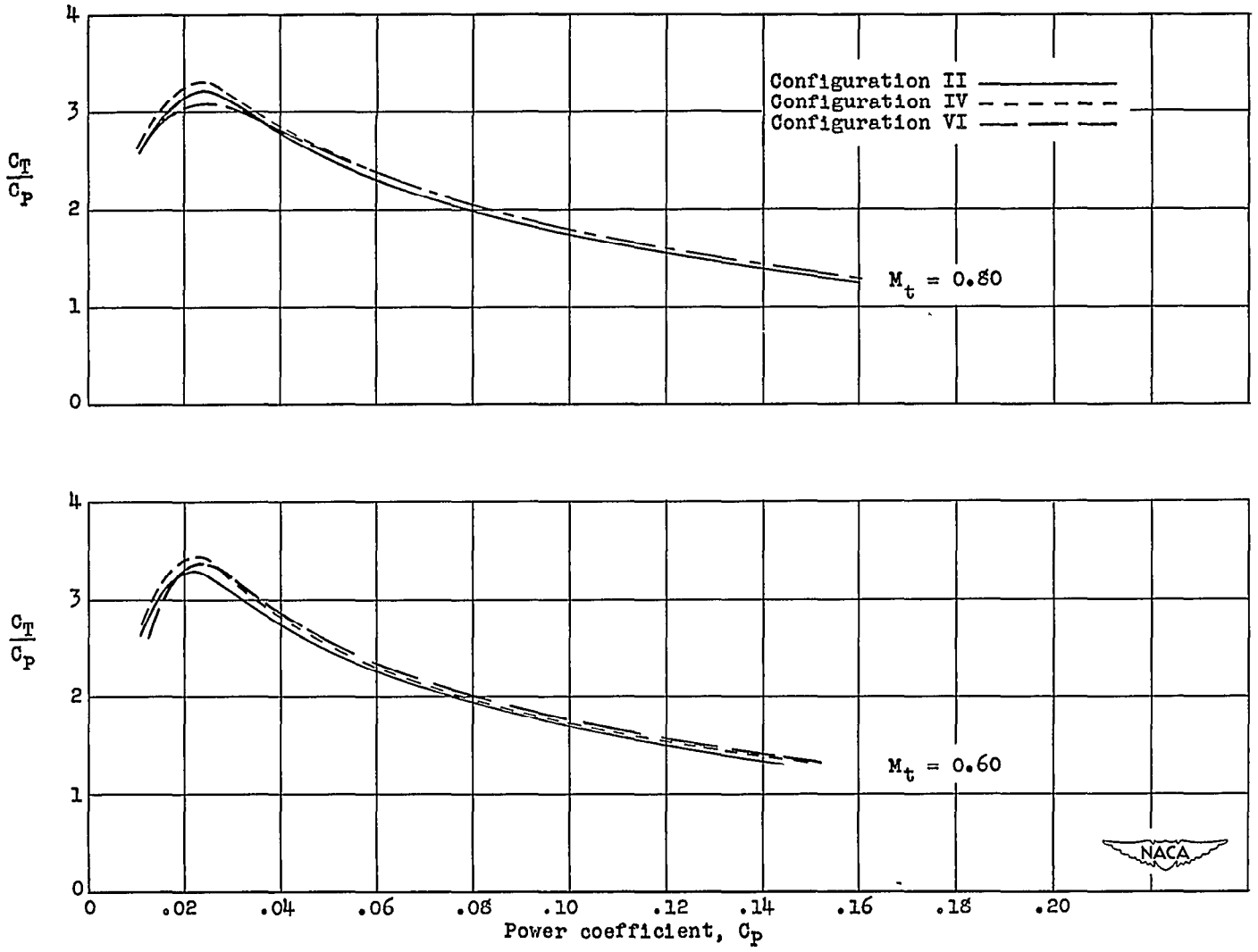

Figure 13.- Variation of static thrust figure of merit with power coefficient at rotational tip Mach numbers of 0.60 and 0.80.

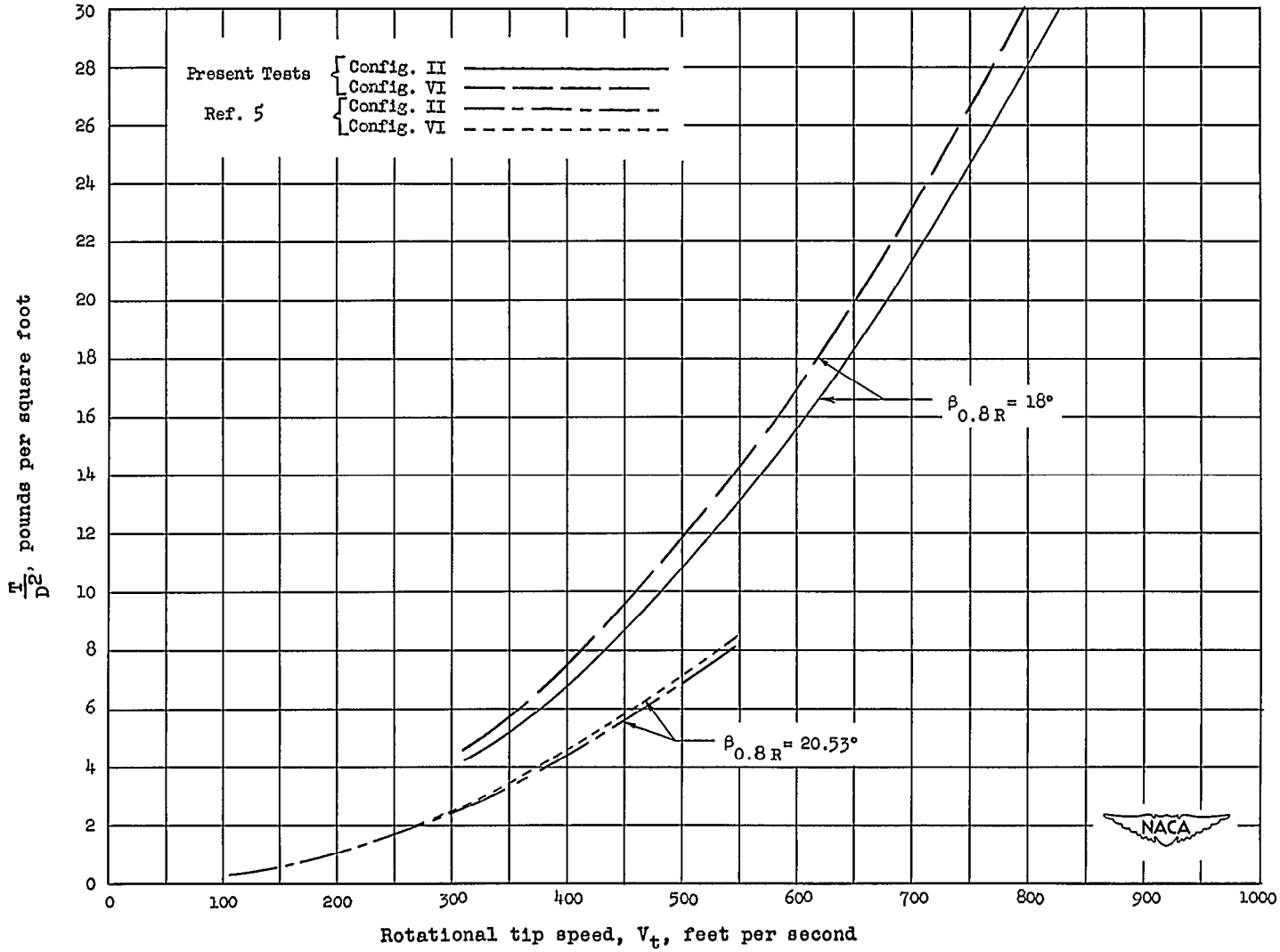

Figure 14.- Variation of T/D^2 with rotational tip speed for present tests as compared with those of reference 5. Tractor configurations.

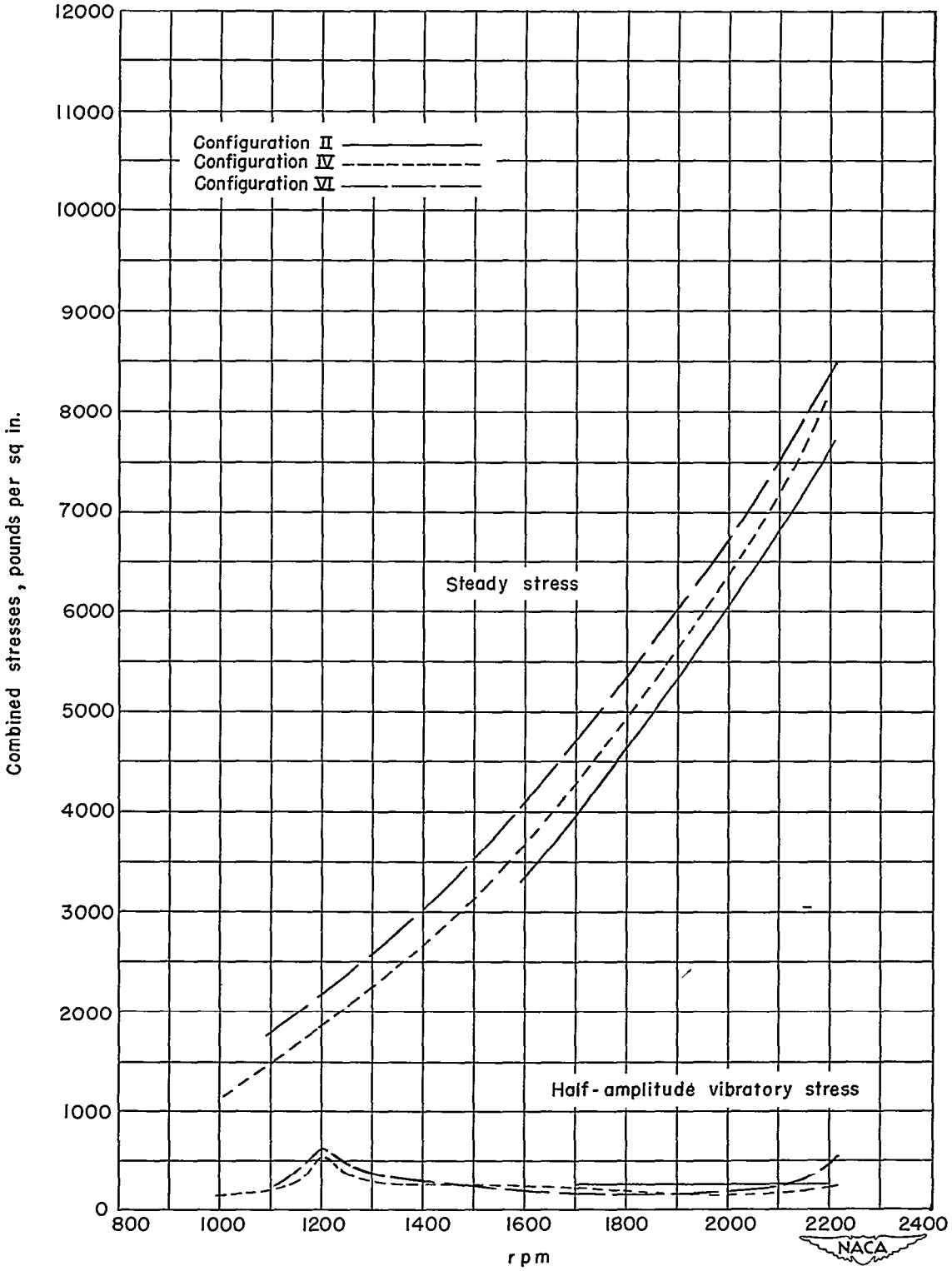

(a) $\beta_{0.75R} = 0^{\circ}$.

Figure 15.- Effect of propeller rotational speed upon combined bending and centrifugal stresses in the propeller blades for the tractor configurations.

CONFIDENTIAL

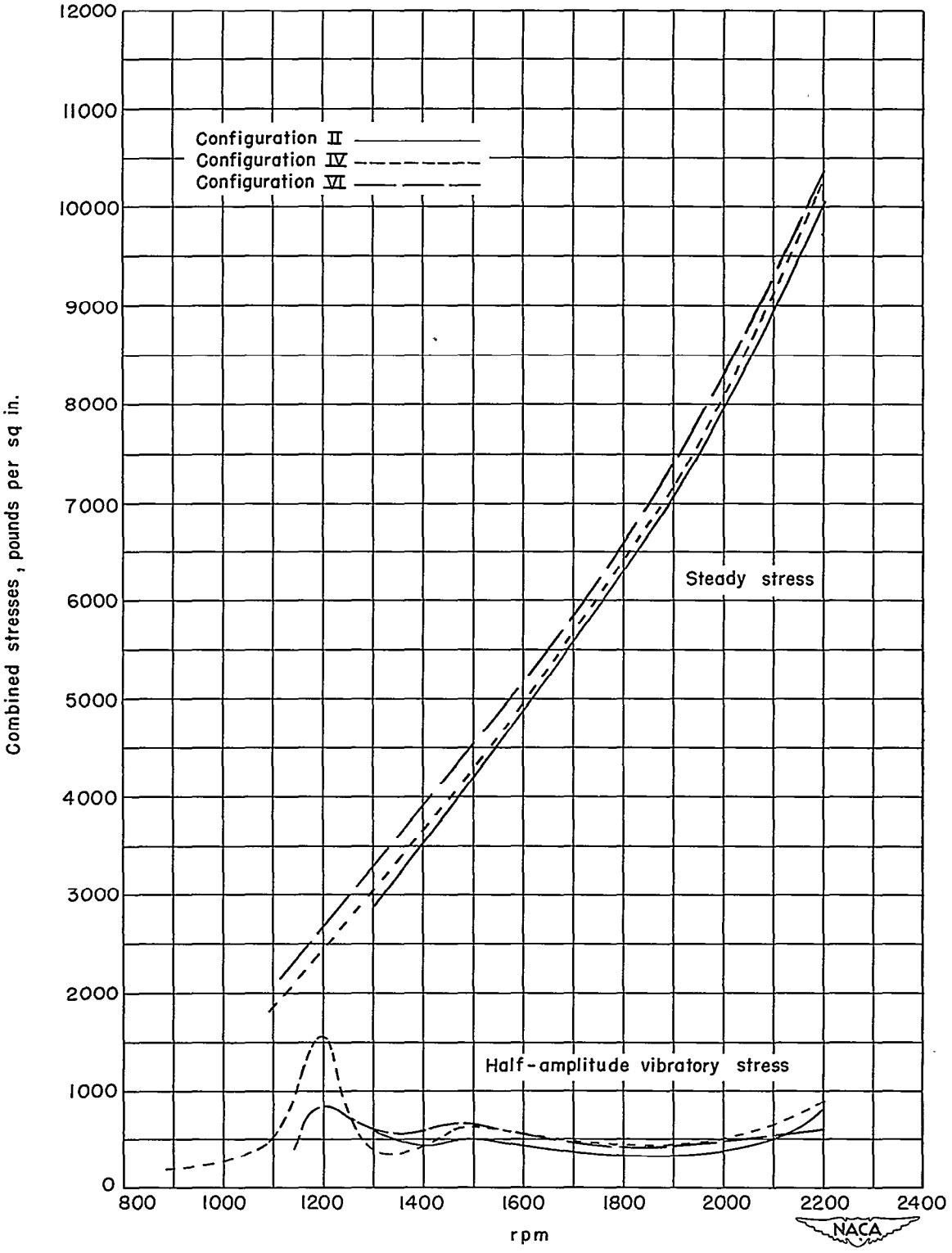

(b) $\beta_{0.75R} = 10^{\circ}$.

Figure 15.- Continued.

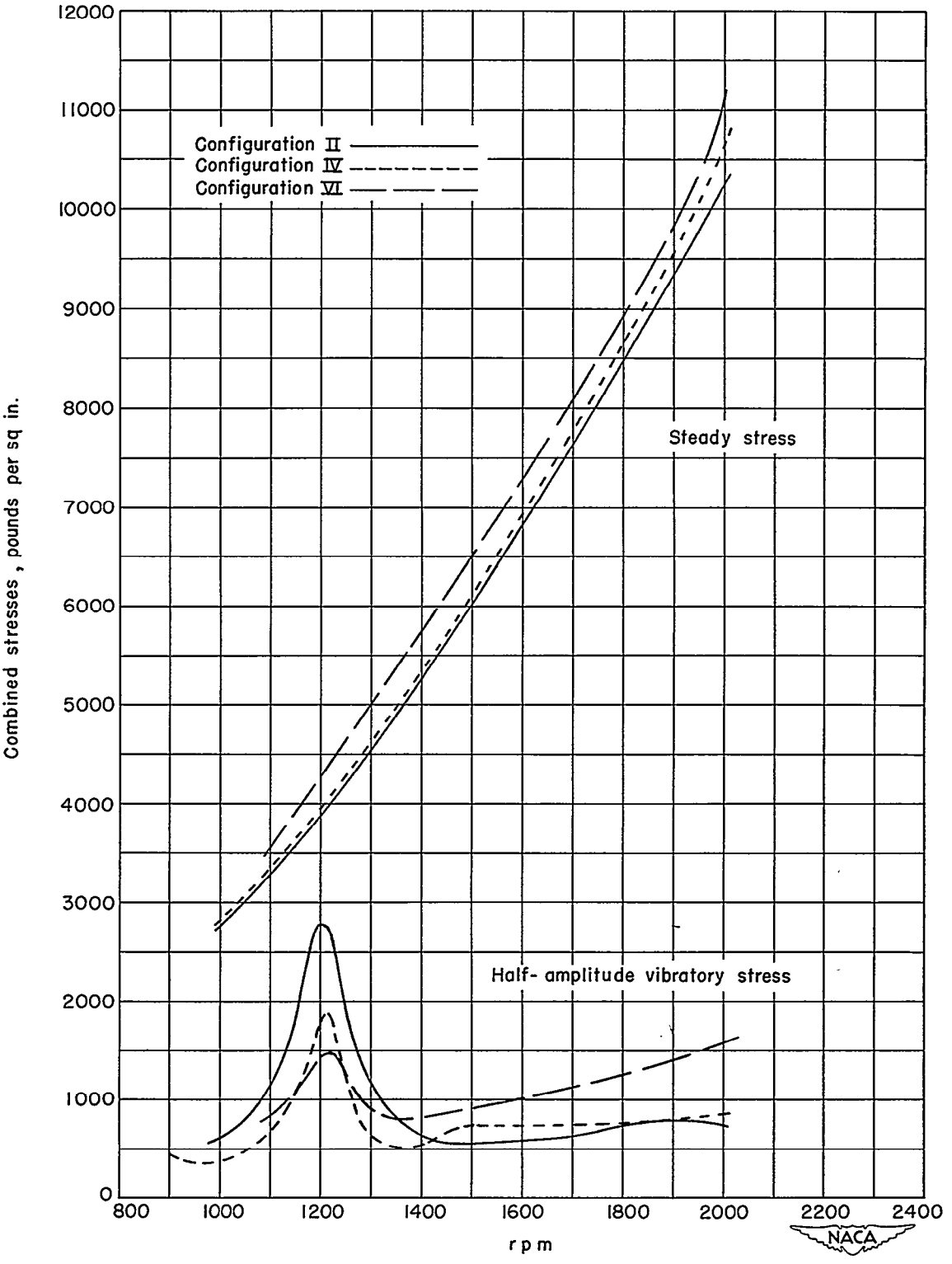

(c) $\beta_{0.75R} = 20^{\circ}$.

Figure 15.- Concluded.

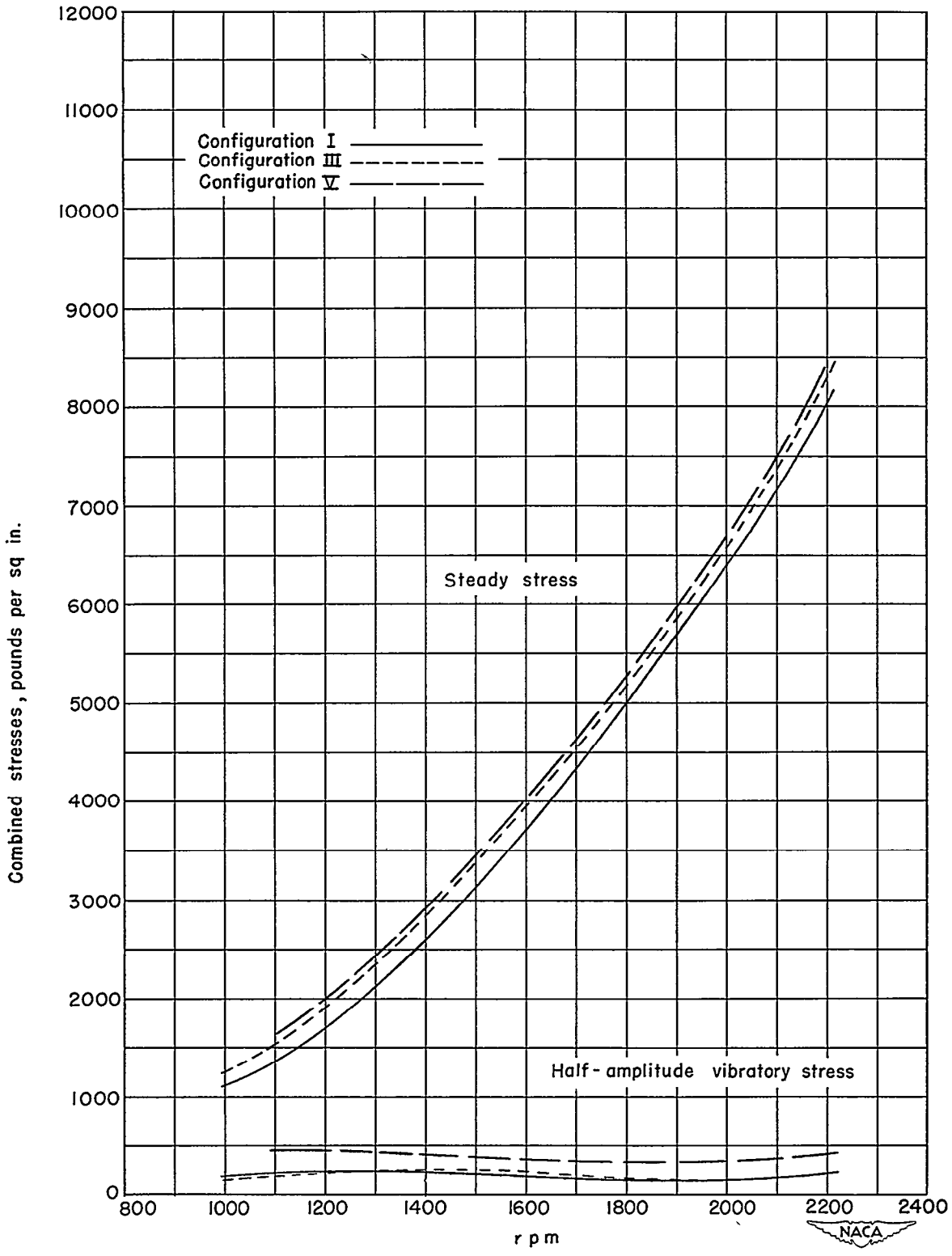

(a) $\beta_{0.75R} = 0^{\circ}$.

Figure 16.- Effect of propeller rotational speed upon combined bending and centrifugal stresses in the propeller blades for the pusher configurations.

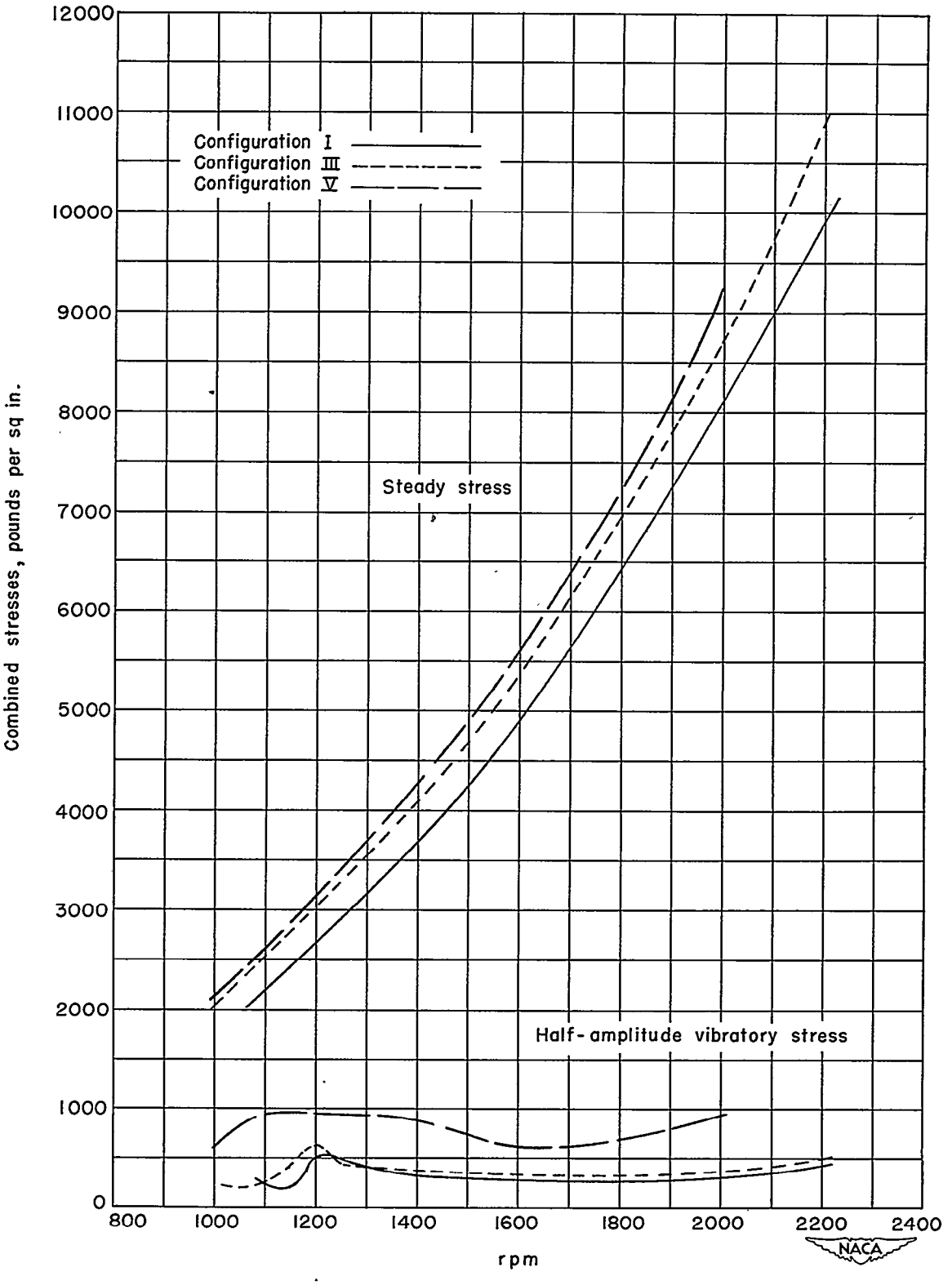

(b) $\beta_{0.75R} = 10^{\circ}$.

Figure 16.- Concluded.